COMPARISON OF TWO OROGRAPHICALLY−ENHANCED PRECIPITATION SYSTEMS OCCURRED AROUND MT. HALLA, JEJU ISLAND, KOREA, DURING RAINY SEASON

5B.2

Keun−Ok LEE, Hiroshi UYEDA
Hydrospheric Atmospheric Research Center, Nagoya University, Japan

Shingo SHIMIZU
Dept. of Storm, flood and landslide Research, National Research Institute for Earth Science and Disaster Prevention, Japan

Dong−In LEE
Dept. of Environmental Atmospheric Sciences, Pukyong National University, Korea

1. INTRODUCTION

In East Asia, most intense precipitation systems occur during the rainy season (June to mid−July), when low−level warm and humid air passing around the Pacific high−pressure flows into the Changma/Baiu/Meiyu front region. Under the moist environment, orographically−enhanced localized heavy rainfalls frequently occur in the vicinity of Mt. Halla (height 1,950 m, width 35 km, length 78 km; Fig. 1) in Jeju Island, southern part of Korea (Lee et al., 2010). Comprehensive understanding of such a regional severe rainfall has been required for developing the quantitative precipitation estimation and mitigating damages arising from flood and landslide around this mountainous area. On 30 June 2006 and 6 July 2007, intense precipitation systems were observed within a dual−Doppler radar observation area showing the system enhancement at the northwestern slope of the island. In this article, the comparison analyses of two intense precipitation systems revealed the vital ingredients for the system enhancement around the narrow but steep topographic feature, such as Jeju Island.

2. DATA AND METHODS

Two operational S−band Doppler radars of Korean Meteorological Administration are located at Gosan (GSN, west) and Seongsan (SSN, east) of Jeju Island with a distance of around 65 km (Fig. 1).

Corresponding author address: Keun-Ok LEE, Hydrospheric Atmospheric Research Center (HyARC), Nagoya Uni., Nagoya, Japan; e-mail: leeko@rain.hyarc.nagoya-u.ac.jp

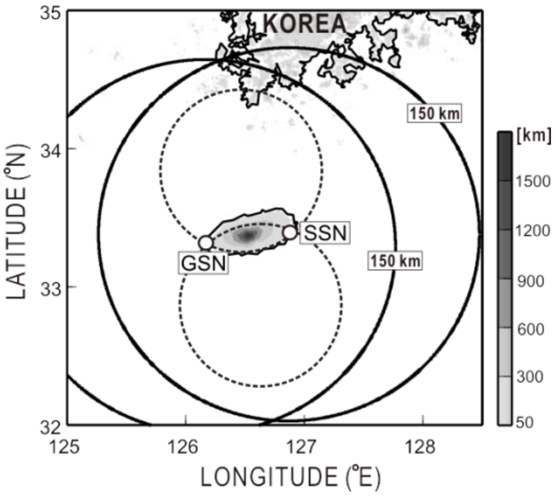

Fig. 1. Elevation map of Jeju Island and observation range (150km; black circle) of the dual−Doppler radars installed at Gosan (GSN) and Seongsan (SSN), which are indicated by small open circles. Dual−Doppler radar analysis was conducted within two dashed circles except for the intersection area (the intersection angle less than 35°).

Each Doppler radar, covering a radius of 250 km around Jeju Island, records sets of volume scans of reflectivity and Doppler velocity (radius of 120 km) every 10 min. The sampling resolution of the radar data is 500 m in the radial direction and 1.0° in the azimuthal direction. Each volume scan consists of 15 elevation angles (0.5° , 0.6° , 0.8° , 1.0° , 1.5° , 2.0° , 2.5° , 3.5° , 4.5° , 6.0° , 7.8° , 10.5° , 13.7° , 18.1° , and 24.0°), although the volume scans obtained before 1330 LST (local standard time; LST = UTC + 9 h) on 30 June consisted of 13 elevation angles (0.5° , 1.5° , 2.5° , 3.5° , 4.5° , 5.5° , 6.5° , 7.5° , 8.5° , 10.0° , 12.0° , 15.0° , and 19.5°). The Doppler radar data was interpolated into a Cartesian coordinate system with vertical and horizontal grid intervals of 0.25 and 1.0 km, respectively. A Cressman−type weighting function was used for the interpolation. To determine the horizontal wind field for 30 June 2006 precipitation system, simplified VVP (velocity volume processing) method (Tatehira and Suzuki, 1994) directly calculated the horizontal component of wind within a volume based on the spatial wind− velocity distribution in the radial direction using GSN data. Since SSN radar started operation from 2007, variational method (Gao et al., 1999) using dual−Doppler radar data was employed to calculate 3−dimensional wind field for the 6 July 2007 precipitation system. Three components of wind in the Cartesian coordinate system were calculated within the dashed circles, except in an intersectant area in Fig. 1 (intersection angle is 35°).

3. RESULTS

3.1 Precipitation system on 30 June 2006

Accumulated rainfall amount of 19 rain gauges across Jeju Island (Fig. 2) indicates that the regional intense rainfall (> 80 mm of rainfall in 100 min) concentrated in the vicinity of the central mountain (Mt. Halla) on 30 June 2006. A part of the result from Lee et al. (2010) was referred in the present study to find the common ingredients enhancing the intense rainfall around Jeju Island by comparison analysis. Upper−air sounding data (data not shown) which was launched at GSN radar site indicated the relatively strong low−level westerly wind (less than 2 km height) blew at around 15 ms^{-1}.

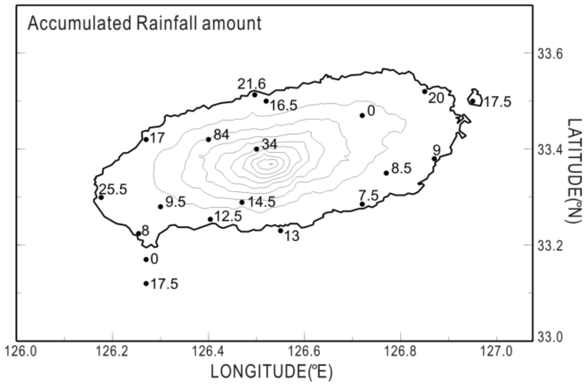

Fig. 2. Accumulated rainfall amount recorded by 19 rain gauges (dots) in Jeju Island from 1320 to 1500 LST on 30 June 2006. Thin contour lines show topography (contour interval: 200 m). *(From Lee et al. (2010))*

The horizontal evolution of the precipitation system on 30 June 2006 (hereafter, ‘06P’) indicated that the eastward−moving convective region (area with reflectivity larger than 45 dBZ) within the system moved from the western to the northeastern island under the predominant westerly wind (Fig. 3). From 1300 to 1330 LST when the convective region approached close to the island from the west offshore (Figs. 3a−d), wind convergence which can be explained by westerly (12 ms^{-1}) and southwesterly winds were found around the northwest of the island at low level. From 1330 to 1350 LST (Figs. 3d−e), the convective region moved from the offshore region to the northwest of the island; in addition, the convective region over the northwestern island increased in size.

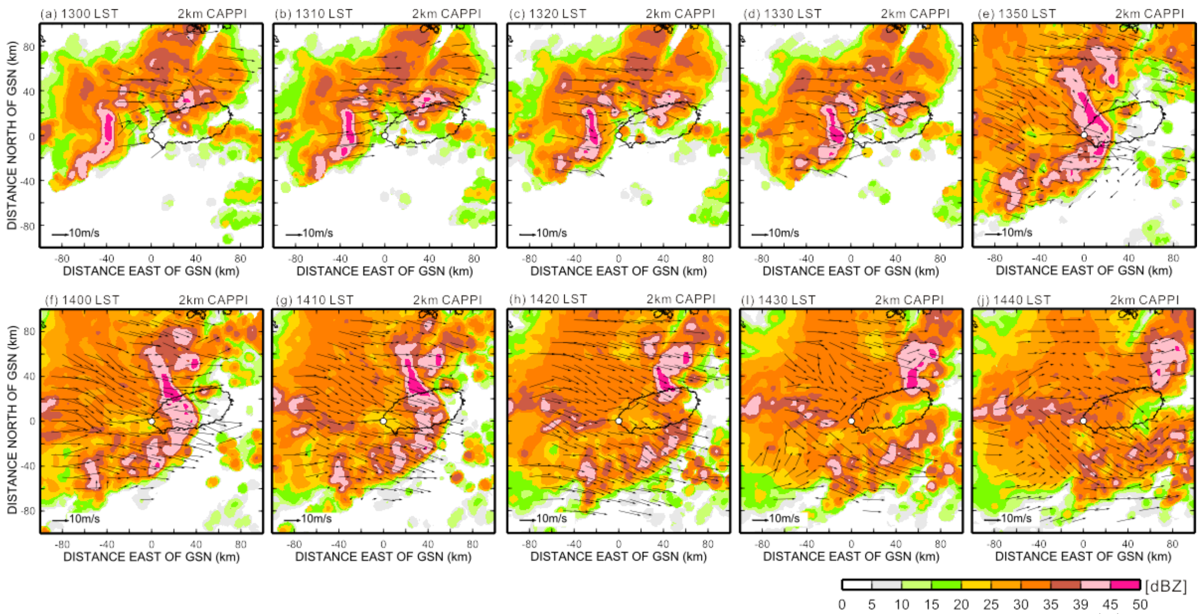

Fig. 3. Horizontal distribution of reflectivity and wind at 2 km ASL and low−level wind vectors for (a) 1300 LST, (b) 1310 LST, (c) 1320 LST, (d) 1330 LST, (e) 1350 LST, (f) 1400 LST, (g) 1410 LST, (h) 1420 LST, (i) 1430 LST, and (j) 1440 LST on 30 June 2006. *(From Lee et al. (2010))*

Subsequently from 1400 to 1420 LST (Figs. 3f–h), the enhanced convective region approached the northern slope and it began to dissipate gradually. At 1430 and 1440 LST (Figs. 3i–j), the 06P was located at the northeastern side of the island, and the convective region was barely discernable within the precipitation system.

To reveal how the topography contributed to the enhancement of the 06P on the northwestern lateral side of the island, control run (CNTL) and no terrain experiment (NOTR) were conducted at 500 m resolution using CReSS (Cloud Resolving Storm Simulator, Tsuboki and Sakakibara, 2002). The result of CNTL showed the localized heavy rainfall amounts exceeding 70 mm in the northwestern slope (Fig. 4) as similar to that shown by the surface rain gauge and radar observation (Figs. 2 and 3). Simultaneously, wind convergence of westerly and southwesterly winds with high relative humidity (RH ~95%) at the northwestern slope of the island (see Lee et al. 2010 for the details).

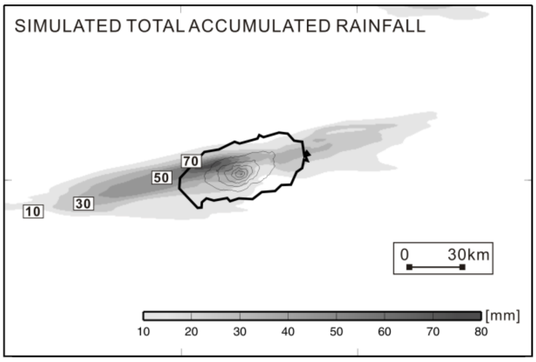

Fig. 4. Simulated total accumulated rainfall amount (grey scale) for 6 hours of CNTL run. Contour lines show the topography of Jeju Island (contour interval: 300 m). *(From Lee et al. (2010))*

Figure 5 shows the difference in total accumulated rainfall amount between CNTL and NOTR simulations (CNTL minus NOTR). Red (blue) areas indicate greater rainfall amount in CNTL (NOTR) than in NOTR (CNTL). The proportion of terrain- produced rainfall amount (positive anomaly) calculated by subtracting the NOTR amount from the CNTL amount, against the rainfall amount produced by CNTL, is 30.6 % (22 mm); in addition, that is found at the northwestern slope of the island. The maximum negative anomaly (18 mm) is seen over the northeastern island, where no orographic blocking occurred, which reflects the horizontal advection of the precipitation system to the lee–side of the island. The effect of orographic blocking generated maximum positive and negative anomalies over the northwestern and

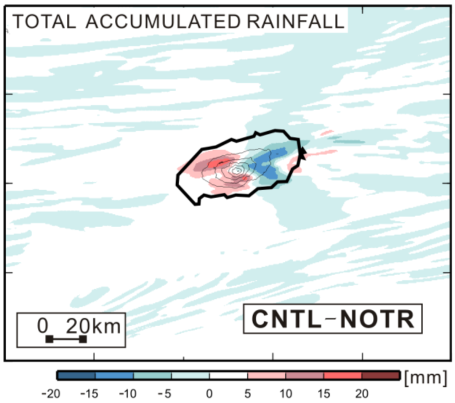

Fig. 5. Distribution of the difference in total accumulated rainfall amount (color scale) between the CNTL and NOTR experiments (CNTL minus NOTR). Black contour lines show the topography of Jeju Island (contour interval: 300 m). *(From Lee et al. (2010))*

the northeastern island, respectively, thereby determining the regional rainfall distribution which was shown in Fig. 2.

3.2 Precipitation system on 6 July 2007

In the similar environment to 06P, an eastward–moving intense precipitation system (hereafter, '07P') was observed with the predominant westerly wind on 6 July 2007. Relatively high rainfall amount of 24 mm and 35 mm was recorded at the north and east island, respectively (Fig. 6). Relatively weak low–level southwesterly to westerly wind around 8 ms^{-1} was found less than 2 km height by the upper–air sounding observation at the GSN radar site (data not shown). To understand the regional rainfall distribution and wind field of 07P, dual–Doppler radar data analyses were conducted.

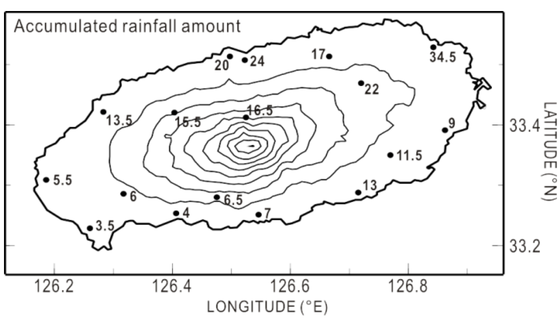

Fig. 6. Accumulated rainfall amount recorded by 17 rain gauges (dots) in Jeju Island from 0000 to 0130 LST on 6 July 2007.

The horizontal reflectivity at 2 km above sea level (ASL) from 0000 to 0130 LST on 6 July 2007 is shown in Fig. 7. From 0000 to 0030 LST (Figs. 7a–d), as an elongated precipitation system moved from the offshore to the northwestern slope of the island, horizontally–enhanced convective region (area with reflectivity larger than 45 dBZ) was found. The farther eastward–moving convective region approached to the northern island and the preserved convective region was observed at 0040 and 0050 LST (Figs. 7e–f). At 0100 LST when the precipitation system located at the northeast island (Fig. 7g), the convective region around 20–30 km north of GSN was persistently shown. In Contrast, relatively dissipated convective region was found around 30–50 km north of GSN. Subsequently, during 0110–0120 LST (Figs. 7h–i), the preserved convective region moved to the east island showing the relatively enhanced convective region at the eastern slope of the island, whereas barely discernable convective region at the northern offshore. At 0130 LST (Fig. 7j), the relatively–dissipated convective region was observed at the eastern offshore of the island.

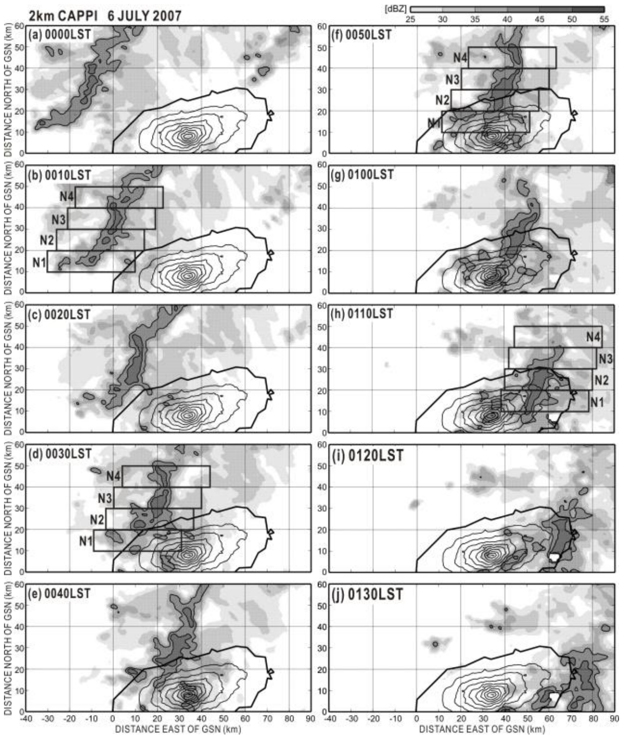

Fig. 7. Horizontal distributions of reflectivity at 2km ASL for (a) 0000 LST, (b) 0010 LST, (c) 0020 LST, (d) 0030 LST, (e) 0040 LST, (f) 0050 LST (upper right), (g) 0100 LST, (h) 0110 LST, (i) 0120 LST, and (j) 0130 LST on 6 July 2007.

To see the difference in evolution of the convective region around Jeju Island, four analysis box **N1** (over mountainous area), **N2** (around the coastal area), **N3** (over near offshore area), and **N4** (over far offshore area) in 40 km × 10 km area were selected so that the convective region could be included (depicted in Fig. 7). The time variation of horizontal area of the convective region of 07P is illustrated in Fig. 8. Figure 8 indicates two significant enhancement of the convective region: 1) at N2 area during 0000–0030 LST and 2) at N1 area during 0100–0130 LST. We analyzed the reflectivity and wind distribution of the system using dual–Doppler radar data, focusing on these two enhancement stages of 07P.

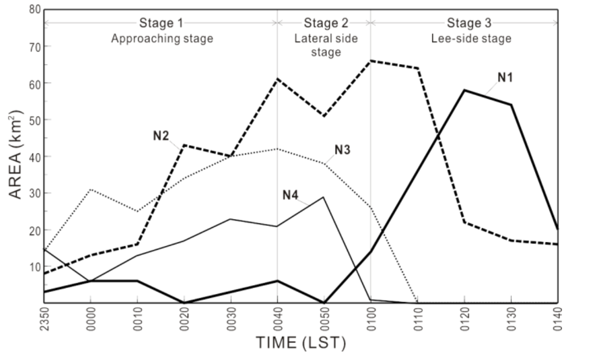

Fig. 8. Time variations of the horizontal area of the convective region (area with reflectivity larger than 45 dBZ) at 2 km ASL within the analysis boxes of N1 (thick solid line), N2 (thick dashed line), N3 (thin dotted line) and N4 (thin solid line) which were depicted in Fig. 7.

The horizontal evolution of reflectivity and wind from 0000 to 0050 LST are illustrated in Fig. 9. Corresponding to the enhancement of the convective region at the N2 area (northwest to north island), strong westerly (20 m s^{-1}), weak southwesterly (7 ms^{-1}) and strong southwesterly (13 ms^{-1}) winds were found at the west, east, and south of the 07P at 2 km ASL (Figs. 9a–e). Simultaneously, the associated updraft region was found at the northwest offshore of the island (Figs. 9g–h), where the predominant westerly was shown at 4 km ASL (Figs. 9l–m). From 0040 to 0050 LST (Figs. 9d–e), the enhanced convective region located around the northern island showing the preserved intensity. Related to the retained convective region at the northern slope of the island, the updraft by the predominant westerly (15 m s^{-1}) and south–westerly (10 m s^{-1}) at the northern slope was analyzed (Figs. 9i–j). Simultaneously, at 4 km ASL (Figs. 9n–o), the predominant westerly was shown around the northern slope of the island.

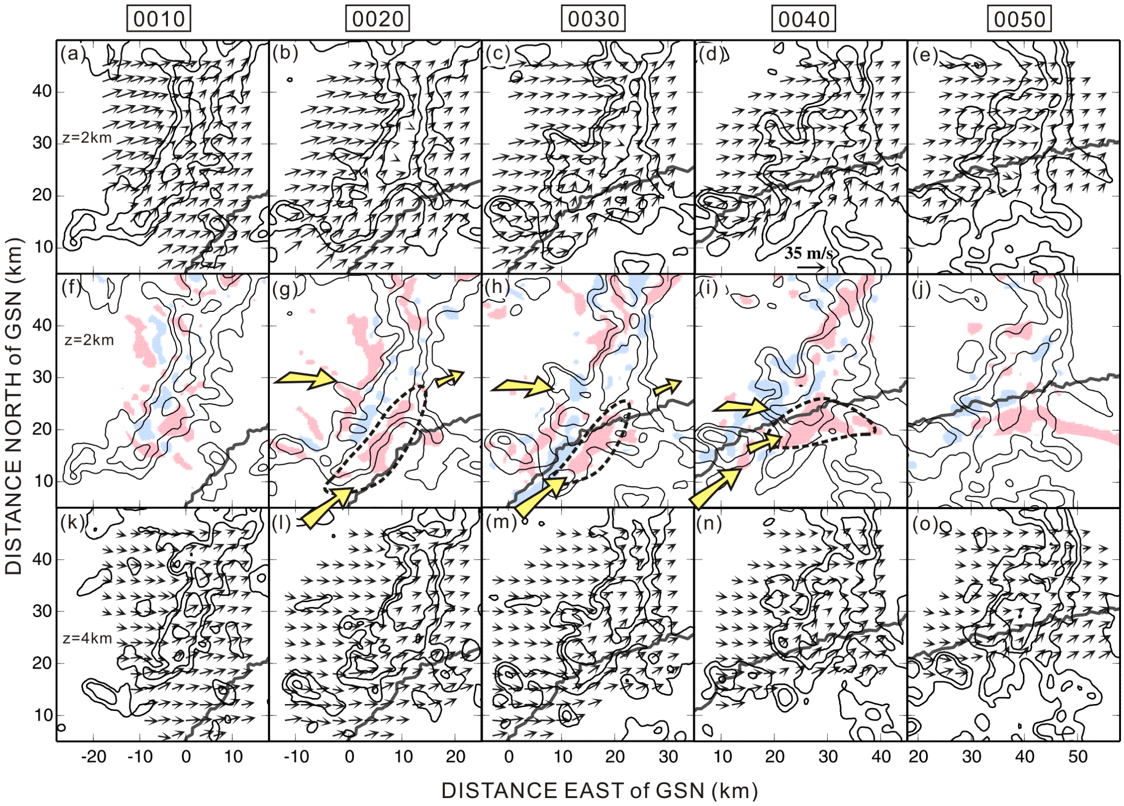

Fig. 9. Horizontal sections of reflectivity and cell−relative wind fields during 0000−0050 LST. The first row (a)−(e) and the third row (k)−(o) show horizontal wind vectors and reflectivity (contour from 35 dBZ at 5 dBZ interval) at 2 km and 4 km ASL, respectively. The second row (f)−(j) shows vertical wind (shadings) at 2 km ASL. Regions of updraft larger than 1.5 $m s^{-1}$ and those of downdraft less than −1.5 $m s^{-1}$ are shaded by red and blue, respectively. Thick contour line in each panel represents coastal line of Jeju Island.

Related to the enhanced convective region at N1, the horizontal evolution of the reflectivity and wind from 0100 to 0130 LST is illustrated in Fig. 10. At 0100 LST (Fig. 10a) when the convective region located at the northeastern side of the island, predominant westerly wind (13 $m s^{-1}$) was found around the convective region. At the same time, relatively strong southwesterly wind (16 ms^{-1}) and its associated updraft were found in the east part of the island at 2 km ASL (Fig. 10d). Subsequently, at 0110 LST (Fig. 10b), the eastward−moving convective region moved to the eastern slope of the island passing over the updraft region, than it significantly enhanced (Fig. 10e). At 0120 LST (Fig. 10c), the enhanced convective region was still found around the eastern coastal area.

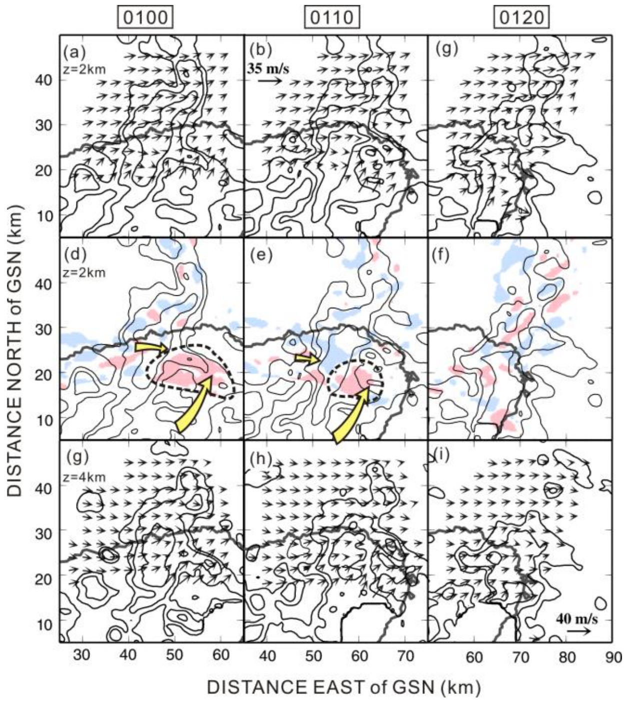

Fig. 10. Same as Fig. 9 but during 0100−0130 LST.

3.3 Comparison of two precipitation systems

The enhancement mechanisms of two intense precipitation systems (06P and 07P) occurred around Jeju Island were investigated and compared.

The common phenomenon of two precipitation systems is that the enhancement of the convective region within the system occurred at the northwestern slope of Jeju Island under the predominant westerly winds. Corresponding to the enhancement, substantial low–level wind convergence which was induced by the westerly and mountain–modified southwesterly winds was concentrated at the northwestern slope with the concentrated low–level moist air.

The different point between two precipitation systems is that the re–enhancement at the lee–side of the mountain was shown in 07P, in contrast, 06P gradually–dissipated as passing around the northern slope of the island. Related to the re–enhancement at the lee–side, the east–southeastward moving convective region of 07P approached to the substantial updraft region at the eastern slope which was generated by the strong southwesterly winds over the southeastern slope. In case of 06P, the convective region moved east–northeastward with the relatively strong low–level southwesterly wind, and its associated downdraft was found at the downwind side at the northeastern slope. Subsequently, the enhanced convective region at the northwestern slope moved to the downdraft region, and it gradually dissipated.

4. DISCUSSION AND CONCLUSIONS

The evolution of convective region (area with reflectivity > 45 dBZ) of intense precipitations occurred on 30 June 2006 (06P) and 6 July 2007 (07P) and the enhancement mechanism were investigated mainly using Doppler radar data. In both precipitation systems, under the low–level moist environment during the rainy season, the convective regions within the systems showed the orographic enhancement at the northwestern slope of the island as the systems approached to the island from the western offshore with the predominant westerly wind. It is inferred that the low–level moist air and predominant westerly wind play an important role enhancing the convective region around Jeju Island.

After the enhanced convective region moved to the northeastern from the northwestern of the island, the evolution of two precipitation systems showed the distinctive phenomena. In east–northeastward passage, the 06P approached to the northeastern slope with the relatively strong low–level wind (15 m s^{-1}). Corresponding to the strong low–level wind, Froude number (*Fr*) was calculated to be 0.55 indicating that the air flows partly could override the mountain (Lee et al., 2010). Indeed, downdraft (w, 0.5 m s^{-1}) was found at the northeastern slope of the island with relatively low RH (less than 84%) and relatively high potential temperature (see Lee et al. (2010) for the details). After the convective region moved to the downwind slope, it subsequently dissipated.

In case of 07P, the enhanced convective region moved to the northern slope of the island where the wind convergence was generated by westerly and terrain–induced southwesterly winds which can supply moist air to the northern side of the island to retain the convective region. In consequence, the retained convective region moved to the eastern slope of the island with the eastward passage and relatively weak low–level wind (~ 10 m s^{-1}). *Fr* of 07P was calculated to be 0.2, indicating that the airflow was unlikely to override the mountain and that it would be affected by the triggering of lee–side convection due to the influence of Mt. Halla (Yoshizaki et al., 2000). Indeed, the updraft region of 07P was found at the eastern slope of Jeju Island where the convective region was significantly enhanced.

06P and 07P showed the different evolution of system enhancement around Jeju Island, under the predominant westerly wind with similar brunt–vaisala frequency (~1.5×10^{-2} s^{-1}) during the rainy season. It seems that the different *Fr* which is induced by the different wind speed of the predominant wind generated the different location of the wind convergence around the narrow but steep mountainous area, such as Jeju Island. In consequence, the downwind region was generated at the northeastern slope of the island to induce the dissipation of the 06P. The relatively weak low–level wind–conducted go–around wind and the related updraft induced the enhancement of the convective region of 07P at the lee–side of the island.

Acknowledgements

The authors thank Dr. C.–H. You of Korea Meteorological Administration for providing the radar data. One of the authors (K. LEE) is supported by the Ministry of Education, Culture, Sports, Science, and Technology, Japan, as a doctoral student in the Graduate School of Environmental Studies, Nagoya University, Japan.

References

Gao, J., M. Xue, A. Shapiro, and K. K. Droegemeier, 1999: A variational method for the analysis of three-dimensional wind fields from two Doppler radars. *Mon. Wea. Rev.*, 127, 2128–2142.

Lee, K.-O., S. Shimizu, M. Maki, C.-H. You, H. Uyeda, and D.-I. Lee, 2010: Enhancement mechanism of the 30 June 2006 precipitation system observed over the northwestern slope of Mt. Halla, Jeju Island, Korea. *Atmos. Res.*, 97, 343–358.

Tatehira, R., and O. Suzuki, 1994: Accuracy in estimation of wind velocity from single Doppler radar (in Japanese). *Tenki*, 41, 761–764.

Tsuboki, K., and A. Sakakibara, 2001: CReSS User's Guide, 2nd edition, 210 pp. [available from http://www.rain.hyarc.nagoyau.ac.jp/~tsuboki/cress_html/src_cress/CReSS2223_users_guide_eng.pdf]

Yoshizaki, M., T. Kato, Y. Tanaka, H. Takayama, Y. Shoji, H. Seko, K. Arao, and K. Manabe, 2000: Analytical and Numerical Study of the 26 June 1998 Orographic rainband observed in Western Kyushu, Japan. *J. Meteor, Soc, Japan*, 78, 835–856.